Inverse correlation between stress response and virulence factor expression in FASII antibiotic-adapted *Staphylococcus aureus* and consequences for infection

Paprapach Wongdontree [1], Aaron Millan-Oropeza [2], Jennifer Upfold [1], Jean-Pierre Lavergne [3], David Halpern [1], Karine Gloux [1], Adeline Page [4], Gérald Kénanian [1], Christophe Grangeasse [3], Céline Henry [2], Jamila Anba-Mondoloni [1], Alexandra Gruss [1*]

[1] Université Paris-Saclay, INRAE, AgroParisTech, Micalis Institute, 78350, Jouy-en-Josas, France. [2] PAPPSO Platform, Université Paris-Saclay, INRAE, AgroParisTech, Micalis Institute, Jouy-en-Josas, France. [3] Bacterial Pathogens and Protein Phosphorylation, Molecular Microbiology and Structural Biology, UMR 5086 - CNRS / Université de Lyon, Building IBCP, 7 Passage du Vercors, Lyon, France. [4] Protein Science Facility, SFR BioSciences, CNRS, UMS3444, INSERM US8, Université de Lyon, Lyon, France

* For correspondence: alexandra.gruss@inrae.fr

Key words: antibiotic adaptation, fatty acid synthesis pathway, virulence factors, oxidative stress, proteome, phosphoproteome, insect infection

Short title: FASII antibiotic adaptation reprograms *Staphylococcus aureus*

Abstract

A crucial step in antimicrobial development pipelines is proof of functionality in the host environment. Antibiotics targeting fatty acid synthesis (FASII) of the major pathogen *Staphylococcus aureus* actively inhibit FASII but do not prevent *in vivo* growth, as bacteria compensate the FASII block by using environmental fatty acids. We report that *S. aureus* responds to FASII antibiotic treatment by major shifts in expression that correlate with improved fitness but decreased virulence, and with altered bacterial killing in an insect infection model. Proteomic kinetics and phosphoproteomic analyses show that anti-FASII provokes massive protein reprogramming compared to non-treated *S. aureus*, while growth is robust in both conditions. Anti-FASII adaptation leads to overall increases in stress response functions and provides greater resistance to peroxide, as produced during host infection. Moreover, *S. aureus* adaptation to anti-FASII is accelerated by pre-treatment with peroxides. In contrast, virulence factor levels are decreased. In keeping with the observed phenotypes, anti-FASII-adapted *S. aureus* are slower to kill their host in a *Galleria mellonella* infection model than non-treated bacteria, but are not eliminated. Thus, anti-FASII adapted cells might be better prepared for survival and less equipped to damage the host. If not eliminated, anti-FASII reprogrammed *S. aureus* populations might provide a bacterial reservoir for the emergence of chronic infections.

Author Summary

Bacterial resistance or adaptation to currently used antibiotics is a main reason for treatment failure. Our work on the major human pathogen *Staphylococcus aureus* revealed that antibiotics targeting fatty acid synthesis (FASII) effectively reach their targets, but do not stop growth. Here we analyzed the expression and infection capacities of *S. aureus* populations that escape anti-FASII inhibition by adapting to the antibiotic. Remarkably, anti-FASII-adapted bacteria show massive expression changes, but grow normally. Once adapted, bacteria produce greater amounts of stress response proteins, while virulence factor levels or activities are lower. Accordingly, anti-FASII-adapted *S. aureus* provoke slower killing in an insect infection model, but bacteria continue to multiply. If not eliminated, anti-FASII reprogrammed *S. aureus* populations could provide a bacterial reservoir for establishment of chronic infections.

Introduction

Staphylococcus aureus is a gram-positive opportunistic bacterium that remains a major cause of disease and mortality in humans and animals. The unsolved crisis of infections due to multidrug-resistance notably methicillin-resistant *S. aureus* (MRSA) underlines the need for alternative treatments, especially in compromised patients (1-4).

Enzymes of the fatty acid (FA) synthesis pathway (FASII) are longtime candidate targets for drug development against *S. aureus* infections (5, 6). FabI was a preferred target as a narrow spectrum inhibitor that would not disrupt the gut microbiome during treatment (7). However, although anti-FASII drugs effectively reach their targets, *S. aureus* growth is not inhibited *in vitro* or in a mouse bacteremia model, as bacteria compensate inhibition by incorporating environmental FAs, as provided by lipid-rich foods and host organs (8-11). Exposure to host lipids during septicemic infection thus favors *S. aureus* adaptation to anti-FASII treatment (10). These studies revealed a caveat for properly testing FASII antibiotic efficacy against Firmicute pathogens such as streptococci, pneumococci, enterococci, and staphylococci. Nevertheless, anti-FASII drug development remains ongoing (12-15).

S. aureus adaptation to anti-FASII treatment is a two-step process involving an initial ~6-8 h latency phase, followed by rapid growth and incorporation of compensatory FAs (**S1 Fig.** (10)). We performed comparative proteomics and phosphoproteomics of non-treated and anti-FASII-treated bacteria to elucidate bacterial expression changes that lead to full adaptation. This study shows that bacteria undergo massive reprogramming during both latency and outgrowth phases of anti-FASII adaptation. A main finding is that *S. aureus* anti-FASII-adaptation leads to an overall increase in stress response, while amounts or activities of virulence factors are decreased. Accordingly, anti-FASII-adapted bacteria caused slowed killing in an insect infection model, but bacteria continued to multiply *in vivo*. Reservoirs of reprogrammed staphylococci emerging after anti-FASII treatment may be a risk factor for chronic infection.

Results

Time-course of *S. aureus* adaptation to anti-FASII by proteomics analyses reveals massive reprogramming. Anti-FASII adaptation in FA-containing serum comprises a latency period followed by vigorous outgrowth (**S1 Fig.;** (10)). Protein profiles of *S. aureus* USA300 during anti-FASII adaptation were determined on OD_{600}-equivalent cultures at 2, 4, 6, 8, and 10 h post-antibiotic treatment. Kinetics were also performed in the absence of serum; in this condition outgrowth takes longer and relies on mutations, mainly in *fabD* (11) (see **S1 Fig.** for growth comparisons). Controls consisted of BHI, FA, and SerFA cultures without triclosan harvested at OD_{600} = ~1. In another control, *S. aureus* was grown in BHI and triclosan (without added FAs), and was harvested 6 h post-treatment. Heat maps of proteome results are based on the means of quadruplicate samples for each condition (see **S1 Table** for complete results and cluster analysis). Compared to the three non-treated controls (BHI, FA, SerFA cultures), massive shifts in protein levels were observed in all anti-FASII-treated samples (**Fig. 1A**). BHI-Tric and FA-Tric samples showed overall decreased abundance, in keeping with poor bacterial viability in the absence of serum. However, serum lowers FA stress and promotes anti-FASII adaptation (10). In this condition, protein reprogramming was detected at the first 2 h post-treatment point.

Condition-specific high-level abundance of *S. aureus* proteins. We inventoried proteins showing the greatest abundance in a single, or a combination of the tested conditions. Proteins showing markedly higher levels in particular conditions are highlighted (**Fig. 1B**, right column): **1-** BHI-Tric resulted in high amounts of FA degradation (Fad) protein FadB. Fad proteins were reported as biochemically non-functional in *S. aureus* (16). However, the *fad* locus is conserved in sequenced *S. aureus* isolates, and transcription is induced in growth-limiting conditions and in the liver (17, 18). BHI-Tric treatment in the absence of exogenous FAs (eFA) might activate Fad as a last-resort means of recycling lipids to provide precursors for survival. **2-** Several highly up-regulated proteins in FA were less produced in SerFA, possibly indicating that FA-induced membrane stress, which is lowered by serum (10, 19, 20), is the induction signal. Proteins comprising the Type VII secretion system were highly FA-induced, as reported (21). Overall lower production of the Type VII proteins in serum-containing medium may

indicate a role for Type VII functions in biotopes where *S. aureus* is stressed by free FAs, but not in sites where serum or host fluids would lower FA toxicity (10, 19, 20). **3-** Levels of FarE, an FA and phospholipid efflux pump (22-24), are highest in FA and FA-Tric conditions. In contrast, FarE levels were low in all serum-containing conditions reflecting decreased membrane stress (10). **4-** Anti-FASII-adapted cells showed high transient or final increases in numerous proteins whose roles remain to be characterized. Protein changes in SerFA-Tric differed strikingly from those in the absence of serum (FA-Tric), where anti-FASII addition stops growth (**S1 Fig.**; (10, 11)). An abrupt increase in biotin synthesis proteins (BioB, SAUSA300_2371; BioA SAUSA300_2372) upon SerFA-Tric outgrowth suggests a strong biotin requirement. Biotin is a required cofactor of the FASII initiation enzyme AccC subunit of acetyl-CoA carboxylase; (SAUSA300_1475 or SAUSA300_1563) and the TCA cycle enzyme pyruvate carboxylase (PycA, SAUSA300_1014) (25). While little change is observed in AccC proteins, amounts of PycA showed a strong increase upon adaptation outgrowth (**S1 Table**). Higher sustained biotin production may contribute to robust growth of anti-FASII-adapted bacteria.

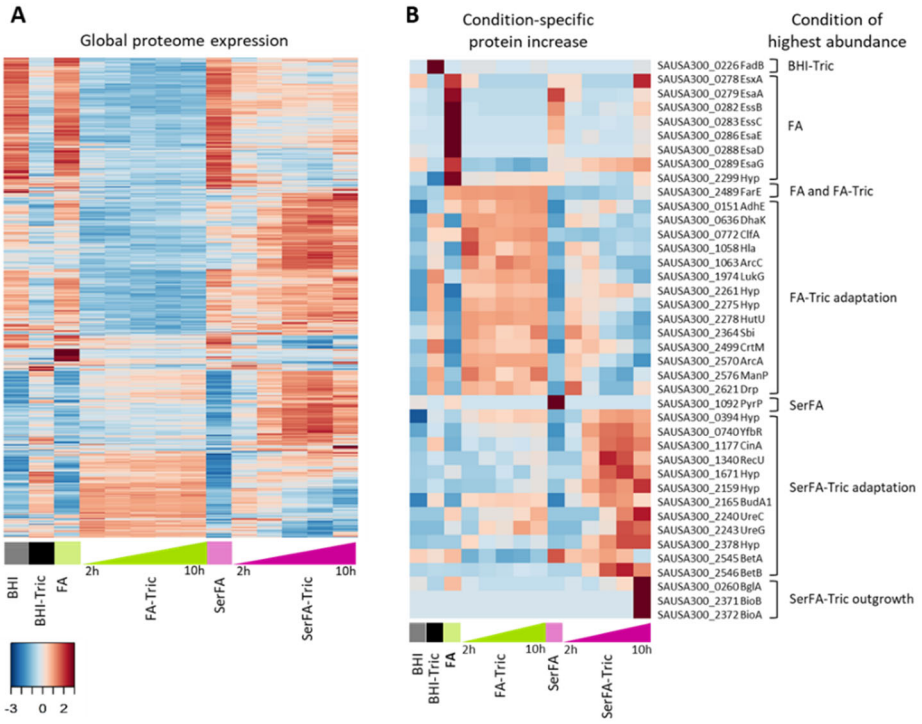

Fig. 1. Expression changes related to *S. aureus* anti-FASII adaptation. Normalized protein expression profiles are organized by growth condition (BHI, FA, SerFA) without and with triclosan (Materials and Methods). **A.** Heat map of global protein changes induced during *S. aureus* adaptation to FASII inhibitor triclosan. **B.** Heat map of condition-specific highly expressed proteins. Proteins listed at right of heat map show high differential expression in conditions indicated after the bracket. Gene names and conditions of highest abundance are at right. FA-Tric and SerFA-Tric kinetics samples were each considered as a group regardless of the time of increased expression. Hyp, hypothetical protein. Color code: Light-to-dark shades of grey, green, and pink represent respectively BHI ± Tric, FA ± Tric, SerFA ± Tric as indicated. Incremental 2, 4, 6, 8, and 10 h time points for FA-Tric and for SerFA-Tric are represented by wedges. The heat map scale is at lower left: representations are calculated as relative protein abundance ratios (red, up-represented; blue, down-represented).

Impact of anti-FASII adaptation on abundance of FASII, FASII-bypass, and phospholipid synthesis proteins. Subsequent analyses focused on anti-FASII effects in serum-containing conditions, as being most relevant to systemic infection. Anti-FASII adaptation affected levels of 16 FASII, FASII-bypass, or phospholipid synthesis proteins (**Fig. 2**). The abundant acyl carrier protein (ACP, AcpP SAUSA300_1125) (estimated at 3655 copies per cell in the *S. aureus* COL strain; (26) and https://aureowiki.med.uni-greifswald.de/SACOL1247) is essential to both FASII and FASII-bypass pathways. Pools of AcpP as well as its modifying enzyme AcpS increased during anti-FASII adaptation. Indeed, most detected lipid synthetic enzymes were present at higher levels throughout SerFA-Tric adaptation compared to untreated cells. After an initial drop in PlsC, a key enzyme for restoring phospholipids *via* FASII bypass, its pools increased gradually during adaptation. Promoter fusion studies previously showed that *plsC* expression is restored during adaptation (27). The increased levels of FASII enzymes in serum-supplemented medium, but not in FA-Tric (**S1 Table**), underline the importance of host factors (here serum) in promoting adaptation (10). We conclude that phospholipid synthesis proteins needed for FASII bypass are maintained or increased in anti-FASII-adaptation conditions.

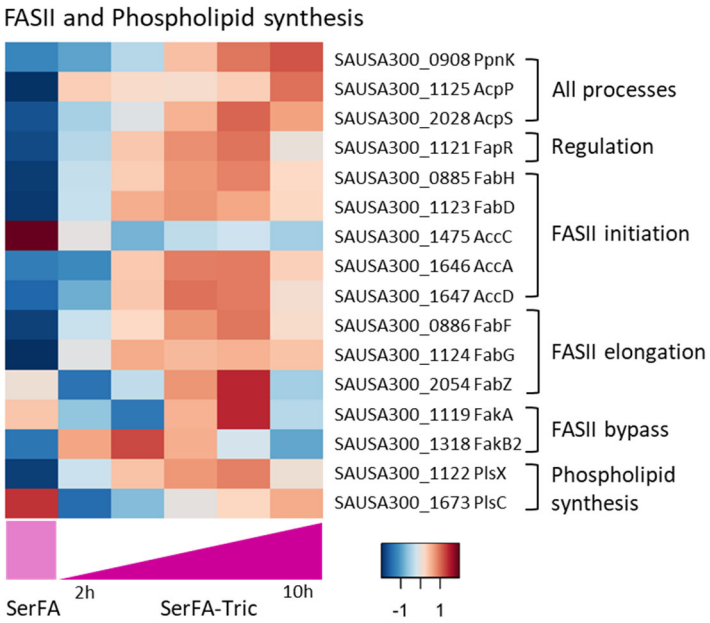

Fig. 2. Heat map of FASII and phospholipid synthesis proteins whose expression is affected in SerFA-Tric growth. Proteins were compiled based on confirmed FASII and phospholipid synthesis pathway proteins. FabI (FASII; SAUSA300_0912) and PlsY (phospholipid synthesis; SAUSA300_1249) were not detected in this proteome. Results are limited to SerFA (control) and SerFA-Tric adaptation conditions. See **S1 Table** for complete test conditions. Gene names and functional categories are at right. Incremental time points for SerFA-Tric 2, 4, 6, 8, and 10 h samples are represented by the wedge. The heat map scale is at lower right: representations are calculated as relative protein abundance ratios (red, up-represented; blue, down-represented).

Increased stress response protein levels and oxidative stress resistance in anti-FASII-adapted *S. aureus*. Levels of 29 / 31 stress response proteins, implicated in pH, osmotic, oxidative, and unfolded protein responses, were transiently or lastingly higher during anti-FASII adaptation and/or outgrowth; just 2 proteins, BetA (SAUSA300_2545) and ClpX (SAUSA300_1621) showed decreased expression (**Fig. 3**). These overall increases may reflect the central role of membrane perturbation in transmitting stress signals. Most heat shock proteins were at least transiently increased during anti-FASII adaptation compared to the control. Heat shock proteins are implicated in *S. aureus* tolerance to a variety of stresses (28). Greater expression of stress response proteins in anti-FASII-treated bacteria might confer a fitness benefit during infection.

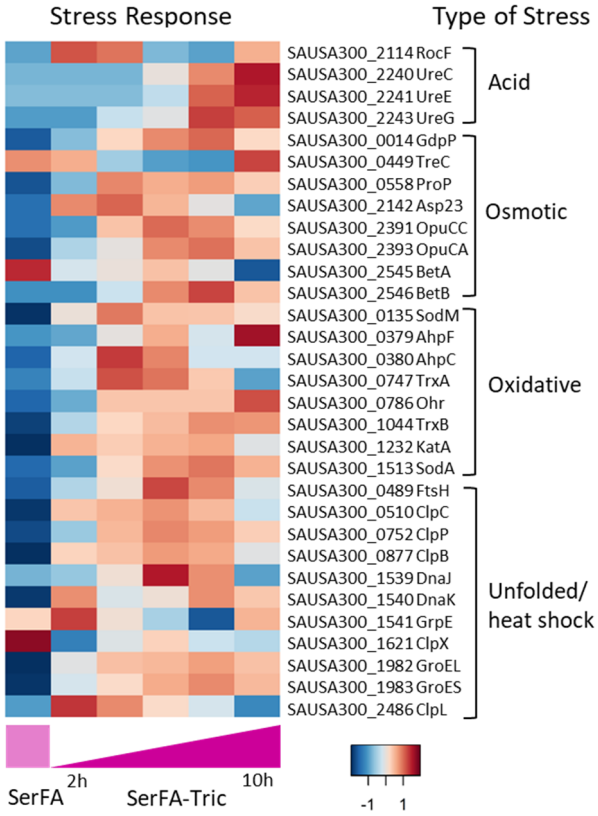

Fig. 3. Stress response proteins are up-expressed during anti-FASII adaptation. Left, heat maps are shown for known or putative stress response proteins. Results are limited to SerFA (control) and SerFA-Tric adaptation conditions. See **S1 Table** for results in all test conditions. Gene names and functional categories are at right. Incremental time points for SerFA-Tric 2, 4, 6, 8, and 10 h samples are represented by the wedge. The heat map scale is at lower right: representations are calculated as relative protein abundance ratios (red, up-represented; blue, down-represented).

As an oxidative burst is part of the host innate immune response to bacterial infection (29), we tested whether anti-FASII adaptation confers a fitness advantage to oxidative stress. Anti-FASII-adapted and non-treated bacteria were compared for their capacity to tolerate H_2O_2 (0.5 mM)

treatment. Compared to non-treated bacteria, anti-FASII-adapted *S. aureus* showed significantly higher tolerance to H_2O_2, as assessed by CFU determinations 5 h after H_2O_2 treatment (**Fig. 4A**).

Pre-treatment with peroxide prior to the anti-FASII challenge enables *S. aureus* adaptation. A study in *Escherichia coli* showed that treating cells with an oxidant led to improved tolerance to fluoroquinolones and other antibiotics (30, 31). To test whether oxidative stress induction contributed to FASII antibiotic adaptation, we primed *S. aureus* with sublethal concentrations of H_2O_2 (0.5 mM) or phenazine-methosulfate (PMS; 20-50 µM) to induce oxidative stress. Bacteria pre-treated or not with the oxidative stress inducers were then tested for anti-FASII adaptation. As anti-FASII, we used the FabI inhibitor AFN-1252, which like triclosan targets FabI, and is a pipeline drug with high specificity (7). Results consistently showed that H_2O_2 and PMS accelerated the time of *S. aureus* adaptation to FASII antibiotics (from 6 to 4-5 hours), compared to non-treated cultures (**Fig. 4B**, **S3 Table**); a *katA* mutant, which lacks catalase and would thus accumulate H_2O_2, adapts to anti-FASII 1 h faster than does the WT parental strain (data not shown). In contrast, treatment with a reducing agent (Na citrate 10 mM, or vitamin C 5.7 mM) had the opposite effects, of retarding adaptation. (**S3 Table**).

Faster adaptation to anti-FASII could be due to up-regulation of an antibiotic efflux pump as reported in *E. coli* (31), or to more rapid adaptation to eFAs. To distinguish between these possibilities, FA profiles were determined 6 h post anti-FASII treatment, when anti-FASII-treated controls are still in latency. Preculturing in H_2O_2 resulted in more efficient eFA incorporation compared to non-pre-adapted cultures (**Fig. 4C**). This strongly suggests that anti-FASII reaches its target, and that ROS pretreatment accelerates eFA incorporation. More efficient incorporation of eFAs in bacteria exposed to H_2O_2 prior to anti-FASII treatment may be linked to a recent report indicating that *S. aureus* respiratory chain impairment favors accumulation of free FAs (32), which could then be incorporated *via* FASII bypass. The mechanisms underlying greater eFA assimilation upon ROS pretreatment is currently under study.

Bacterial pathogens are known to trigger stress responses in infected host macrophages and neutrophils (33, 34). The efficacy of anti-FASII drugs to eliminate *S. aureus* from infected host cells might thus be adversely affected by the oxidative stress response mounted by the host.

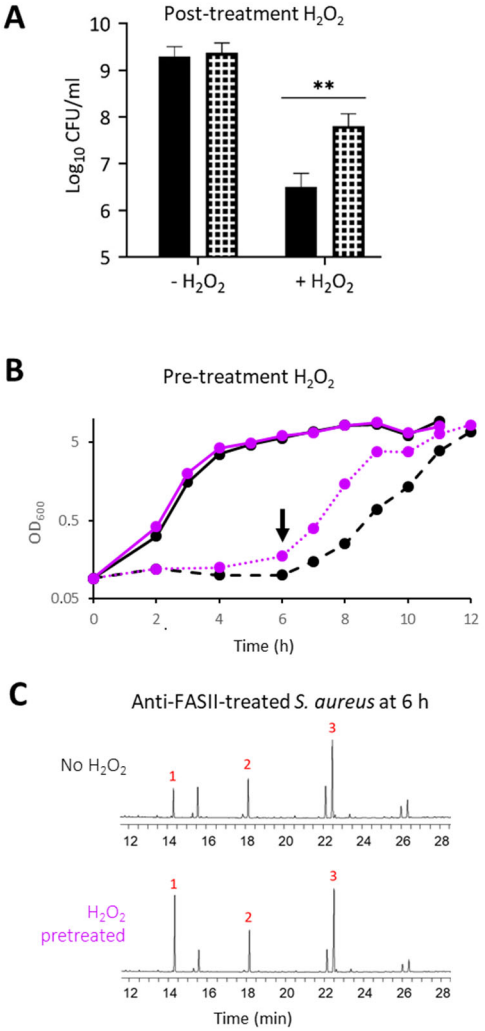

Fig. 4. H_2O_2 primes bacteria for accelerated adaptation to anti-FASII. A. *S. aureus* anti-FASII adaptation leads to increased H_2O_2 resistance. USA300 non-treated (black bar) and AFN-1252-adapted cultures (hatched bar) issued from overnight growth were challenged with 0.5 mM H_2O_2. CFUs of surviving bacteria and controls were determined after 5 h incubation. **, p≤ 0.01. **B** and **C.** Priming *S. aureus* with H_2O_2 accelerates anti-FASII adaptation. **B.** USA300 cultures were grown overnight in SerFA without or with 0.5 mM H_2O_2. Cultures were diluted to OD_{600} = 0.1 and grown without or with 0.5 µg/ml AFN-1252. OD_{600} was monitored for 12 h. Growth curve is representative of 4 independent experiments. Black, no pretreatment; purple, pre-treatment with H_2O_2. Solid lines, SerFA, dashed lines SerFA-AFN. **C**. FA profiles were done twice independently on cultures harvested after 6 h anti-FASII treatment (arrow in '**B**'). 1, 2, and 3, eFAs added to cultures (respectively C14, C16, and C18:1). H_2O_2-primed cultures incorporate more eFAs than unprimed cultures. See Materials and Methods for protocols.

Reduced levels and activities of virulence factors in anti-FASII-adapted *S. aureus*. Unlike the higher expression of stress response proteins, levels of 10 out of 16 detected virulence-related proteins (*e.g.* adhesins, Fe or heme binding proteins, and toxins) decreased transiently or lastingly during anti-FASII adaptation compared to non-treated *S. aureus* cultures (**Fig. 5A**). In addition, we evaluated major secreted virulence factors not detected by proteomics: hemolysin, lipase, nuclease, and protease (**Fig. 5B**). SerFA day precultures were subcultured in SerFA without or with two tested anti-FabI drugs, triclosan (in SerFA-Tric) and AFN-1252 (in SerFA-AFN). The appropriate detection plates were then spotted with 10 µl overnight cultures, whose optical densities were similar (OD_{600} = 13, 9, and 9,

respectively in non-treated, triclosan-adapted, and AFN-adapted conditions). Activities of all 4 exoproteins were visibly lower in both anti-FASII-adapted cultures compared to non-treated cultures.

Taken together, these results indicate that the altered *S. aureus* state during anti-FASII-adaptation favors greater resilience to host stress by raising levels of stress response proteins, but lowers host killing capacity by reducing virulence factor production. These features may prepare anti-FASII-treated *S. aureus* for greater persistence in the host, effective at least during the time of antibiotic treatment.

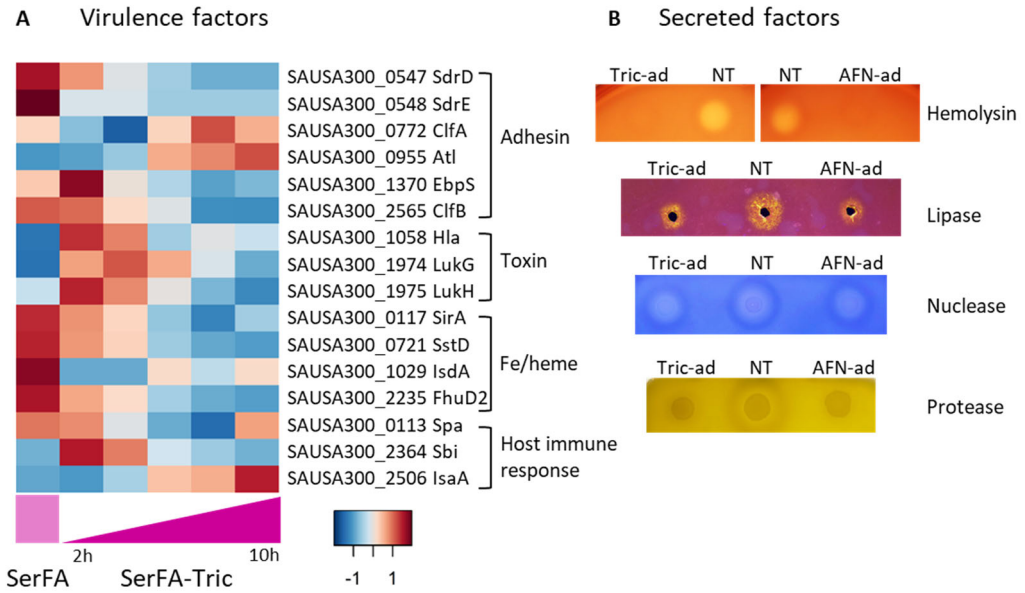

Fig. 5. Decreases in virulence factor levels and activities in anti-FASII adapted *S. aureus*. A. Heat maps are shown for known virulence factors. Results are limited to SerFA (control) and SerFA-Tric adaptation conditions. See **S1 Table** for results in all test conditions. Gene names and functional categories are at right. Incremental time points for SerFA-Tric 2, 4, 6, 8, and 10 h samples are represented by the wedge. The heat map scale is at lower right: representations are calculated as relative protein abundance ratios (red, up-represented; blue, down-represented). **B.** Secreted virulence factor activities. Non-treated (NT) and anti-FASII-adapted cultures using Triclosan (Tric-ad) or AFN-1252 (AFN-ad) were grown overnight, and reached similar OD_{600} values (= 13, 9, and 9 respectively for NT, Tric-ad, and to AFN-ad). Cultures (for protease detection) and culture supernatants (hemolysin, lipase, and nuclease detection) were evaluated (see Materials and Methods). A representative result of 3 biologically independent replicates is shown.

Expression and phosphorylation of regulatory proteins are re-directed during anti-FASII adaptation. We anticipated that regulatory changes dictate the reprogramming induced by anti-FASII treatment. Our assessment revealed 22 documented or predicted regulators whose expression decreased (9 proteins) or increased (13 proteins) during anti-FASII adaptation (**Fig. 6**). Identified regulators affect stress response, nutritional immunity, metabolism, and virulence, or combinations of these factors. It is notable that nearly all regulator levels reached peak changes during adaptation, and then returned

to baseline, suggesting that induced changes are transient. Two exceptions, CcpE and CshA, peaked at outgrowth and thus may be candidates for maintaining anti-FASII adaptation (discussed below).

Moreover, regulators are often modulated by post-translational modifications and/or intracellular metabolites, thus complicating elucidation of their roles. As phosphorylation has documented effects on protein regulators (35-37), we also performed phosphoproteome analysis, in which we compared bacterial modifications in non-treated conditions (OD_{600} = 1), and after 6 h and 10 h of anti-FASII treatment by triclosan (**Table 1**, **S2 Fig.**; **S2 Table** for full results).

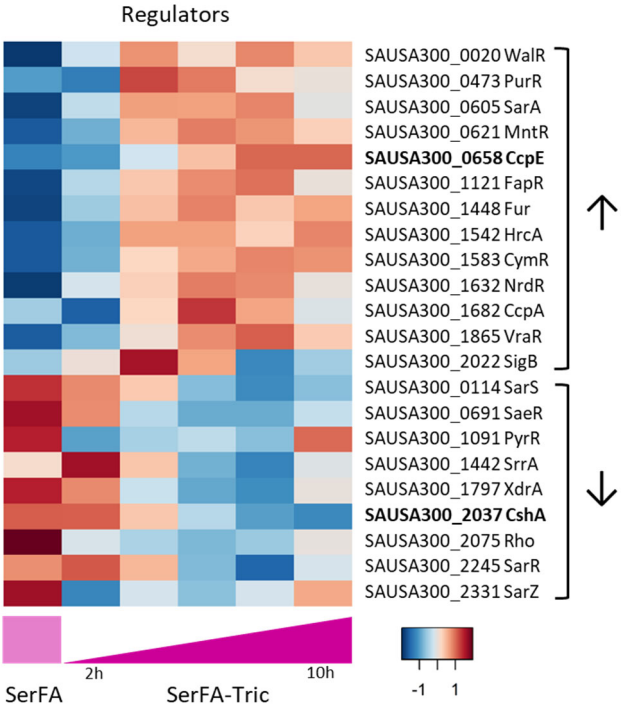

Fig. 6. Regulatory proteins showing expression reversal in anti-FASII compared to non-treated cultures. Heat maps are shown for known or putative regulators in public databases and were curated manually. Results are limited to SerFA control and SerFA-Tric adaptation conditions (see **S1 Table** for results in all test conditions). The greatest changes in most regulatory protein levels were visible at 6 and 8 h during the latency phase of anti-FASII adaptation. Gene names are at right. Incremental time points for SerFA-Tric 2, 4, 6, 8, and 10 h samples are represented by the wedge. The heat map scale is at lower right: representations are calculated as relative protein abundance ratios (red, up-represented; blue, down-represented). Regulators in bold displayed lasting shifts in anti-FASII adapted bacteria.

Here we focus on regulators whose phosphorylation is impacted by anti-FASII adaptation (see (38) for a comprehensive *S. aureus* phosphoproteome in non-selective conditions). Altogether, 7 regulators affected for protein levels and/or phosphorylation upon anti-FASII adaptation are discussed; the difficulties in interpreting their roles are pointed out.

i- FapR (SAUSA300_1121) is a main regulator of FASII and phospholipid synthesis, which affects *fabD*, *fabH*, *fabF*, *fabG*, *fabI*, *plsX*, and *plsC* ((39), although *plsC* control is indirect (27)). FapR expression increased up to 6-fold compared to the SerFA control during adaptation. However, FapR repression is alleviated by malonyl-CoA binding (39). During anti-FASII adaptation, malonyl-CoA preferentially

interacts with FapR, such that FASII, but also phospholipid synthesis proteins needed for anti-FASII adaptation, are increased (27). Thus, increased FapR levels may not cause greater FapR repression.

ii- CshA (SAUSA300_2037) is a well-characterized DEAD-box helicase and part of the RNA degradosome complex (40). CshA impacts membrane FA homeostasis in *S. aureus*; Pdh operon mRNA, a CshA target, is not degraded in a *cshA* mutant, so that acetyl-CoA pools are increased (41). Anti-FASII adaptation led to a progressive lasting decrease in CshA pools, suggesting that acetyl-CoA pools are increased in this condition (**Fig. 6;** (27)). ACC uses acetyl-CoA to produce malonyl-CoA, the FapR anti-repressor (42). In parallel, levels of ACC subunits AccD and AccA (SAUSA300_1646 and 1647) increased during anti-FASII adaptation (**Fig. 2**). Thus, decreased CshA and consequent increased acetyl-CoA (*via* PDH) and malonyl-CoA (*via* ACC) may contribute to anti-FASII bypass by upregulating the FapR regulon.

iii- HrcA (heat-inducible transcription repressor; SAUSA300_1542) represses expression of heat shock proteins DnaJ, DnaK and GroEL (43). Both HrcA levels and phosphorylation increased in anti-FASII adaptation (**Fig. 6, Table 1**), while amounts of HrcA-regulated heat shock proteins also increased (**Fig. 3**). We suggest that phosphorylation may derepress HrcA to activate heat shock protein expression.

iv- Rot (regulator of toxins; SAUSA300_1708; (44)) showed increased phosphorylation upon *S. aureus* adaptation to anti-FASII that was pronounced at 10 h. During anti-FASII adaptation, responses of Rot-regulated functions, hemolysin, lipase, protease are decreased, while Spa is increased (**Fig. 5**), as expected when Rot is active, suggesting that Rot phosphorylation reinforces repressor activity. In contrast, levels of ClfB, which is reportedly activated by Rot, is strongly decreased, indicating that other regulators or metabolites control its expression.

v- XdrA (SAUSA300_1797) is implicated in capsule synthesis, biofilm formation and virulence factor expression (45-47). The first gene in the FA degradation (*fad*) operon, *fadX*, is repressed by XdrA (46). Consistently, transcriptomics performed across multiple conditions showed that the *fad* operon is upregulated while *xdrA* is down-regulated in growth-limiting conditions (17). Both the amounts and phosphorylation of XdrA decreased during anti-FASII treatment. It is possible that *fad* upregulation when XdrA pools are lower directs FAs towards Fad-mediated degradation, which would transiently

limit FA availability for FASII bypass. This proposed role for XdrA in shunting eFAs between FASII bypass and degradation remains to be tested.

vi- CcpE (LysR family transcriptional regulator; SAUSA300_0658) is a positive regulator of the TCA cycle that is activated by citrate. *CcpE* mutants display greater virulence, linked to higher pigment production, iron capture, and resistance to killing (48). CcpE is increasingly produced and is underphosphorylated during anti-FASII adaptation. Higher CcpE levels may favor growth at the expense of virulence-related factors in this condition.

vii- SaeR (DNA-binding response regulator; SAUSA300_0691) is the response regulator of a two-component system that mediates expression of some 20 virulence factors. Sae signaling is activated by hydrogen peroxide (49). It is turned off by free FAs in a *fakA* mutant, and by anti-FASII, as also observed here in response to triclosan (50). Thus FA stress, as may occur in *fak* mutants, and membrane perturbation provide signals or metabolites that turn off SaeRS transcription. Supporting this, the membrane-disrupting lipopeptide colistin also lowers *saeRS* transcription (17).

Taken together, this study identifies several regulators implicated in anti-FASII adaptation. It leads us to suggest that membrane perturbations (here induced by anti-FASII) may constitute a primary signal leading to regulatory adjustments. These results provide a basis for determining how these regulators interactively rewire *S. aureus* expression during anti-FASII adaptation.

Infection by untreated and anti-FASII-adapted *S. aureus* in the *Galleria mellonella* infection model. The significant expression changes related to anti-FASII treatment led us to ask whether infection capacity is affected in anti-FASII-adapted *S. aureus*. We chose an insect *G. mellonella* model for testing, which allowed us to use a large cohort and thus assess overall changes due to anti-FASII. It is notable that larval hemocoel, like blood serum, is lipid-rich (51). The anti-FabI antibiotic AFN-1252 was chosen for this study, as it was extensively tested for treatment of *S. aureus* infections, and was pharmacologically vetted for non-toxicity in the host (16, 52). Non-treated and AFN-1252-adapted *S. aureus* USA300 showed equivalent kinetics when grown in SerFA *in vitro* (**S3 Fig.**). Insects were injected with 10^6 CFU non-treated or AFN-1252-treated *S. aureus* USA300; a control group was injected with

PBS (Materials and Methods). Two experiments, using 140 and 130 insects were performed, respectively to assess insect survival (**Fig. 7A**), and bacterial CFUs in insects (**Fig. 7B** and **C**), with monitoring at 0, 24, 48, and 72 h post-infection. Insects infected by anti-FASII-adapted bacteria were killed more slowly than those infected by untreated bacteria. At T_{48}, 95% of insects were killed by untreated *S. aureus*, compared to 30% killing with anti-FASII-adapted *S. aureus*. At T_{72}, when all larvae infected by untreated *S. aureus* were dead, mortality in the group infected with anti-FASII-adapted *S. aureus* increased to 64%. Thus, killing by anti-FASII-adapted *S. aureus* was delayed but not stopped.

At T24, *S. aureus* counts on SerFA solid medium were comparable in the two infected insect groups. After that time CFUs from surviving insects infected by anti-FASII-adapted bacteria decreased (**Fig. 7B**). In contrast, CFUs in dead larvae at T_{48} were comparable for both groups, indicating that anti-FASII adapted bacteria multiplied as well as non-treated bacteria in the insects they killed (**Fig 7C**).

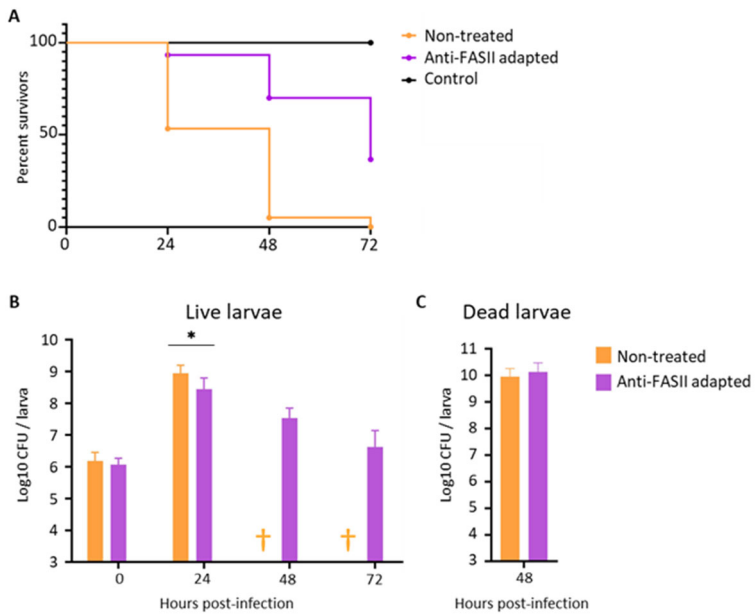

Fig. 7. Comparison of untreated and anti-FASII-treated *S. aureus* in a *G. mellonella* infection model. *S. aureus* cultures were prepared as described in Materials and Methods. Ten microliters were injected per insect. **A.** Insect survival in non-treated and anti-FASII-adapted *S. aureus*. Data was analyzed using Kaplan-Meier with pooled values of biologically independent triplicates (60 samples per condition). A Mantel-Cox test was done on results excluding the PBS controls, and showed a significance value of $p < 0.0001$. **B.** Bacterial CFUs in insects infected by non-treated and anti-FASII-adapted *S. aureus* in surviving insects. †, no surviving insects. *, $p \leq 0.05$. **C.** Bacterial CFUs in insects infected by non-treated and anti-FASII-adapted *S. aureus* in dead insects at 48 h. '**B**' and '**C**' analyses were done using the non-parametric Mann Whitney test using Graphpad prism software.

To determine whether anti-FASII-adapted bacteria remained adapted during infection, CFU platings as above were done in parallel on SerFA-AFN solid medium. Only anti-FASII-adapted bacteria grow directly on SerFA-AFN medium (**Table 2**). Among surviving insects infected with adapted bacteria, only one contained bacteria that returned to the non-adapted state at 72 h; this indicates that bacteria can remain adapted during infection (**Table 2**). Altogether, these results show that anti-FASII-adapted *S. aureus* are able to kill their host. Consistent with proteomic results, anti-FASII-adapted *S. aureus* populations are less virulent, but maintain their capacity to withstand host conditions.

Discussion

Anti-FASII treatments against *S. aureus* infection are in continued development, based largely on protocols using short intervals between infection and antibiotic treatment challenge (14, 15, 53, 54). Our work stressed the importance of antibiotic testing in real-life conditions, *i.e.*, in which treatment is administered *after* palpable signs of infection. This strategy would reduce risks of pursuing false leads in drug development. Importantly, *S. aureus* adapts to anti-FASII in these conditions and then grows robustly, thus advising against its use as single-drug treatment (10).

The present work shows that anti-FASII-adapted *S. aureus* populations undergo massive and lasting expression shifts that improve bacterial tolerance to hostile conditions while reducing damage to the host (**Fig. 8**). During infection, the host elicits an inflammatory response upon infection, including ROS production (55). Paradoxically, pre-exposure to an oxidative stress favors *S. aureus* adaptation to FASII antibiotics and accelerates eFA incorporation, while growth with a reducing agent slows adaptation (**S3 Table**). We speculate that bacteria exposed to the host inflammatory response would more readily overcome anti-FASII inhibitors as seen here *in vitro*. In *E. coli*, pre-exposure to ROS leads to greater antibiotic tolerance by reducing proton-motive-force-mediated entry or by inducing efflux pump expression; this is at least partly due to induction of an Fe-S repair system (30, 31, 56). In the case of anti-FASII, H_2O_2 pre-treatment accelerates FA incorporation in *S. aureus*, proving that anti-FASII reaches its target, and implying that a different mechanism is involved. A role for Fe-S proteins in modulating FA incorporation is under current study.

We observed a major shift in regulator protein levels in anti-FASII adapted bacteria (**Fig. 7**). However, we failed to uncover a master regulator responsible for the massive shift in expression. Numerous protein regulators are modulated by metabolites and/or post-translational modifications (27). Indeed, phosphoproteomics revealed differential phosphorylation of 4 regulators, involved in iron, stress response, toxin expression, and biofilm production, which may explain at least in part the phenotypic changes observed during anti-FASII adaptation (**Table 1**). We previously showed that CodY (SAUSA300_1148), the conserved central amino acid- and GTP- responsive regulator, was required for

normal anti-FASII adaptation (57). In *S. aureus*, CodY intervenes in FASII and phospholipid regulation (27), acts on other regulators to repress virulence factor production (58), and controls expression of acid-stress-response urease genes, some of which are upregulated upon anti-FASII adaptation (**Fig. 4**; (59)). Although changes in CodY levels were not detected by proteomics, a *codY* mutant is severely delayed for anti-FASII adaptation (27), indicative of a central regulatory role. While the above observations illustrate the complexity of interpreting proteomic findings, our findings will serve as a basis for determining how the identified regulators modulate anti-FASII adaptation.

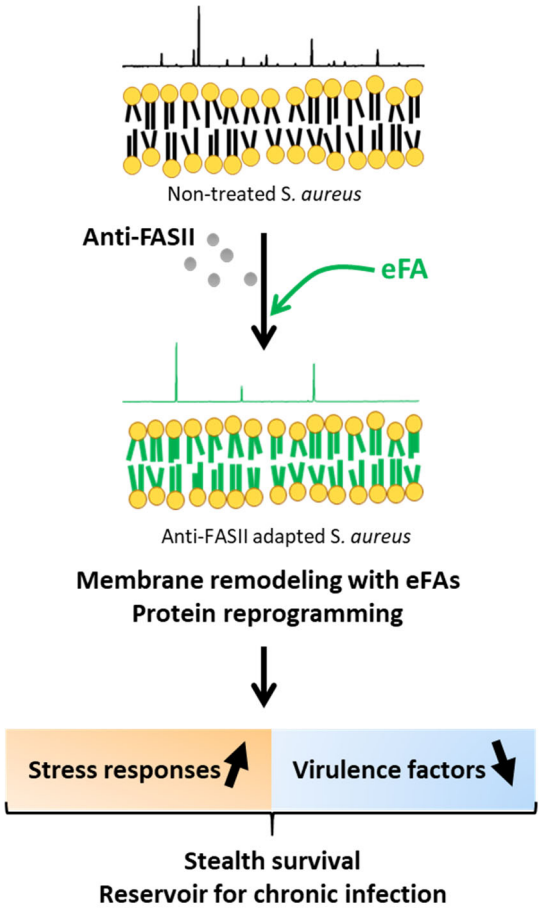

Fig. 8. Consequences of anti-FASII on *S. aureus* adaptation. Non-treated *S. aureus* synthesizes fatty acids (FAs) used to produce membrane phospholipids. A typical gas chromatography FA profile of *S. aureus* grown in laboratory medium (black line) is shown above a depiction of the membrane. Addition of anti-FASII in SerFA medium results in a replacement of self-synthesized FAs by the eFAs (here C14, C16, C18:1; green line depicts bacterial profile), and an exogenous membrane phospholipid composition. Anti-FASII adaptation is accompanied by massive changes in protein expression. Notably, increases in numerous stress response proteins may help bacteria cope with host-produced ROS (55). Decreased virulence factor production may help bacteria avoid induction of the host immune response (60). Reservoirs of anti-FASII-adapted *S. aureus* may give rise to chronic infection in the host.

To our knowledge, inverse stress and virulence factor responses were not previously linked to other antibiotic treatments, and may be specific to anti-FASII adaptation, or to drugs that induce membrane perturbations. Some parallels exist between features of anti-FASII-adapted bacteria and those of small colony variants (SCVs), which are associated with chronic infection: both emerge more efficiently in oxidative stress (**Fig. 4**, **S3 Table** (61, 62)), and both produce less virulence factors (**Fig. 5**; (60, 63)),

which might facilitate bacterial escape from host immune surveillance. In contrast, tricarboxylic acid cycle enzymes are less produced in SCVs (64), but not in anti-FASII-adapted *S. aureus*, whose outgrowth kinetics in SerFA medium was comparable to that of untreated bacteria (**S3 Fig.**). We propose that anti-FASII-adapted *S. aureus* generate a bacterial reservoir potentially leading to chronic infection (**Fig. 7**).

Although anti-FASII fails to eliminate *S. aureus* when compensatory fatty acids are available, the present study shows that it does reduce *S. aureus* virulence factor production. Anti-FASII may synergize with other treatments that prevent adaptation and thus potentiate its efficacy (27). Here, anti-oxidants delayed anti-FASII adaptation (**S3 Table**), which may offer perspectives for a bitherapy approach to eliminate *S. aureus* with attenuated virulence.

Materials and Methods

Strains, media, and growth conditions. Experiments were performed using *S. aureus* SAUSA300_FPR3757 JE2 strain, referred to below as USA300, or a *katA* SAUSA300_1232 transposon insertion mutant ((65); generously supplied by BEI Resources NIAID, NIH, USA). All cultures were grown aerobically at 37°C. Solid and liquid growth media were based on BHI as follows: no additives (BHI), containing 0.5 mM FAs (BHI-FA, with an equimolar mixture of 0.17 mM each C14, C16, C18:1 [Larodan, Sweden]), and BHI-FA containing 10% newborn calf serum (Ser-FA; Eurobio Scientific, France [Fr]). Where specified, the anti-FASII triclosan (66) was added at 0.25 µg/ml in media without serum, and at 0.5 µg/ml in media containing serum, to respectively give BHI-Tric, FA-Tric, or SerFA-Tric, as described (10, 11, 67). The anti-FASII AFN-1252 (7) was used in SerFA at 0.5 µg/ml (SerFA-AFN) as described (10). For most experiments, *S. aureus* USA300 was streaked on solid BHI medium, and independent colonies were used to inoculate overnight BHI pre-cultures. For proteomic and phosphoproteomic studies, cultures were inoculated at a starting OD_{600} = 0.1. Where indicated, SerFA precultures contained hydrogen peroxide (0.5 mM final concentration).

Proteomics preparation and analyses. Adaptation to anti-FASII varies with growth media: BHI-Tric-grown and FA-Tric-grown *S. aureus* do not adapt in the time periods tested, (high frequency adaptive mutations arise with a delay in FA-Tric; (11)), whereas SerFA-Tric-grown *S. aureus* adapt without mutation after an initial latency period (6-8 hours, depending on growth conditions) (10). Kinetics experiments were performed on USA300 to determine the protein changes associated with FA-Tric and SerFA-Tric anti-FASII adaptation. Cultures for each condition were prepared as independent quadruplicates. For each sample, BHI precultures were diluted and shifted to the specified medium starting cultures at OD_{600} = 0.1. Control cultures in BHI, BHI-FA and BHI-SerFA were grown to OD_{600} = ~1. BHI-Tric cultures (no added FAs) were collected at 6 h. USA300 samples grown in FA-Tric and SerFA-Tric were collected at 2, 4, 6, 8 and 10 h post-antibiotic addition (see **S1 Table** for growth information and complete data). For each sample, 20 OD_{600} units culture equivalent was collected and centrifuged for 10 min at 4°C at 8000 rpm. Pellets were washed twice in Tris 10mM pH7.0 containing 0.02% TritonX-

100, and Halt™ Protease & Phosphatase Inhibitor Cocktail (100X) (Thermo Scientific, Fr). Pellets were then resuspended in 650 µl washing buffer, mixed with 0.1 mm silica beads and subjected to 3 cycles of vigorous shaking (Fast-Prep-24, MP-Bio, Fr). After 10 min centrifugation at 10000 rpm, supernatants were recovered and stored at -80°C prior to analyses.

Protein extractions, LC-MS/MS analyses, and bioinformatics, and statistical data analyses were done as described in detail (68). The reference genome GenBank Nucleotide accession code NC_007793.1 was used for protein annotation. The bioinformatic tools used for proteomics analysis (X!TandemPipeline C++, MassChroQ, MCQR) are open and free resources available in the following repository: https://forgemia.inrae.fr/pappso. The mass spectrometry proteomics data was deposited to the ProteomeXchange Consortium (http://proteomecentral.proteomexchange.org) via the PRIDE partner repository with the dataset identifier PPXD034256.

Proteome data analyses. Protein abundance differences were detected by ANOVA tests for all methods used (spectral counting, SC; extracted ion chromatograms, XIC; and peak counting, PC). The abundance of a protein was considered significantly variable when the adjusted p-value was <0.05. Proteins showing significant statistical abundance differences were represented on heat maps using hierarchical clustering with Euclidean distances as described (68). K-means clustering analysis was performed using RStudio. Proteins whose abundancies were significantly different in one or more conditions were manually curated and classified according to functional groups.

Phosphoproteome preparation and analyses. USA300 cultures were prepared in BHI and SerFA and harvested at OD_{600} = ~1. SerFA-Tric cultures were harvested at 6h and 10 h post-treatment. Samples were prepared independently from those in the proteomics study, as independent biological triplicates, and treated as in proteomics studies, except that we collected the equivalent of 50 OD_{600} units. Bacteria were processed as for proteome extraction except that Tris was replaced by triethylammonium bicarbonate (50 mM; *n.b.* Tris interferes with dimethyl tag labelling) containing antiprotease and antiphosphatase at the recommended concentrations. Lysed bacteria after Fast-Prep

were centrifuged 15 min at 12000 rpm supernatants containing soluble proteins were kept at -80°C before use. Protein concentrations were determined by the Bradford method.

One mg protein samples were evaporated and resuspended in 1 ml 5 % formic acid and dimethyl-tag labeled as described (69). Briefly, differential on-column labeling of peptide amine groups (NH_2) created dimethyl labels leading to mass shifts of +28.0313 Da for the peptides from SerFA 3 h samples, +32.0564 Da for the peptides from SerFA-Tric 6 h samples and +36.0757 for the peptides from SerFA-Tric 10 h samples respectively. The three samples were mixed and then submitted to six rounds of phosphopeptide enrichment with 5mg TiO_2 beads/mg of protein (Titansphere Phos-TiO, GL Sciences Inc., Netherlands) as described (70).

LC-MS/MS analyses of samples were done using an Ultimate 3000 nano-RSLC coupled on line with a Q Exactive HF mass spectrometer (Thermo Scientific, San Jose California). 1 µL of each sample was loaded on a C18 Acclaim PepMap100 trap-column 300 µm inner diameter (ID) x 5 mm, 5 µm, 100Å, (Thermo Scientific) for 3.0 minutes at 20 µL/min with 2% acetonitrile (ACN), 0.05% TFA in H_2O and then separated on a C18 Acclaim Pepmap100 nano-column, 50 cm x 75 µm ID, 2 µm, 100 Å (Thermo Scientific) with a 100 minute linear gradient from 3.2% to 20% buffer B (A: 0.1% FA in H_2O, B: 0.1% FA in ACN), from 20 to 32% of B in 20 min and then from 32 to 90% of B in 2 min, hold for 10 min and returned to the initial conditions. The flow rate was 300 nL/min.

Labeled peptides were analyzed with top15 higher energy collisional dissociation (HCD) method: MS data were acquired in a data dependent strategy selecting the fragmentation events based on the 15 most abundant precursor ions in the survey scan (m/z range from 350 to 1650). The resolution of the survey scan was 120,000 at m/z 200 Th and for MS/MS scan the resolution was set to 15,000 at m/z 200 Th. For HCD acquisition, the collision energy = 27 and the isolation width is of 1.4 m/z. The precursors with unknown charge state, charge state of 1 and 5 or greater than 5 were excluded. Peptides selected for MS/MS acquisition were then placed on an exclusion list for 20 s using the dynamic exclusion mode to limit duplicate spectra. The mass spectrometry proteomics data have been deposited to the Center for Computational Mass Spectrometry repository (University of California, San

Diego) *via* the MassIVE tool with the dataset identifier MassIVE MSV000089781 (accessible at http://massive.ucsd.edu/ProteoSAFe/status.jsp?task=db3f5002e32e4a47a71996358bc6ae8c).

Phosphoproteome data analyses. Proteins were identified by database searching using SequestHT with Proteome Discoverer 2.5 software (Thermo Scientific, Fr) against the Uniprot *S. aureus* USA300 database (2020-01 release, 2607 sequences). Precursor mass tolerance was set at 10 ppm and fragment mass tolerance was set at 0.02 Da, and up to 2 missed cleavages were allowed. Oxidation (M), acetylation (Protein N-terminus), and phosphorylation (S, T, Y) were set as variable modifications. The dimethyl labeled peptides in primary amino groups K and N-ter (+28.0313 Da for the SerFA 3h sample, +32.0564 Da for the SerFA-Tric 6h sample and +36.0757 Da for the SerFA-Tric 10 h sample), and carbamidomethylation (C) were set as fixed modifications. Peptides and proteins were filtered with a false discovery rate (FDR) at 1% using the Percolator tool (71). Protein quantitation was performed with precursor ions quantifier node in Proteome Discoverer 2.5 software, peptide and protein quantitation based on pairwise ratios and t-test statistical validation.

H_2O_2 resistance of non-treated and anti-FASII adapted *S. aureus*. *S. aureus* non-treated or AFN-adapted cells (see above) were diluted to OD_{600}= 0.005 in SerFA and grown for 1 h at 37°C, after which H_2O_2 (0.5mM final concentration) was added or not to cultures, and allowed to grow for 5 h. Growth kinetics was followed by OD_{600} determinations, and CFUs were determined at the final time point. Plates were photographed after overnight incubation at 37°C.

H_2O_2 and PMS pre-treatment. For pre-adaptation in hydrogen peroxide or in PMS, *S. aureus* were precultured in SerFA and then subcultured in SerFA containing or not 0.5 mM H_2O_2 (final concentration) or PMS (20-50 µM) for 16 h at 37°C. Cultures were diluted to OD_{600} = 0.1 in SerFA or SerFA medium containing AFN-1252 (SerFA-AFN), and growth was monitored.

Nuclease detection assay. DNase agar (Oxoid, Thermo Scientific, Fr) containing toluidine blue O 0.05 g/L (Sigma, Fr) was prepared as described (72). Culture supernatants from test samples were heated to 80°C for 10 m, and then spotted (10 µl) on plates. Photographs were taken after overnight

incubation at 37°C. Contrast was uniformly enhanced by Photoshop to visualize pink halos indicating nuclease activity.

Protease activity assay. Powdered skim milk 50 g/L was added to 1% non-nutrient agar (Invitrogen). Medium was sterilized at 121°C for 15 min as described (73). Cultures were spotted (10 µl) on plates and allowed to dry, then incubated at 37°C for 72 h and photographed.

Lipase activity assay. Medium comprised 1% non-nutrient agar (Invitrogen) to which was added 2.5% olive oil and 0.001% Rhodamine B (starting from a Rhodamine B stock solution of 1 mg per ml in water; Sigma-Aldrich, Fr) as described (74). To improve olive oil emulsification, NaCl was added to medium (1M final concentration), followed by vigorous shaking just prior to plate preparation. Supernatants from overnight cultures were sterile-filtered through a 0.2 µm membrane syringe filter (Pall Corporation, Michigan). Supernatants (10 µl) were deposited in holes pierced in solid medium. After 24 h incubation at 37°C plates were visualized under UV light at 312 nm and photographed.

Hemolytic activity assay. *S. aureus* sterile-filtered supernatants were prepared from overnight cultures and 10 µl aliquots were spotted on 5% sheep blood agar plates (BioMérieux SA, Fr). After drying, plates were incubated at 37°C overnight, and photographed.

***G. mellonella* infection by anti-FASII-adapted and untreated *S. aureus*.** Infection capacities of anti-FASII-adapted and untreated *S. aureus* USA300 were compared in the *G. mellonella* insect model (75). *G. mellonella* larvae were reared on beeswax and pollen in sealed containers with a wire mesh lid permitting aeration. The rearing container was stored at a constant temperature of 27°C in a humidified incubator in our laboratory facilities. The fifth instar larvae weighing ~250 mg were subjected to starvation for 24 h at 27°C and 1-2 h at 37°C prior to infection. *S. aureus* SerFA cultures were subcultured in SerFA, and SerFA plus AFN-1252 (0.5µg/ml; SerFA-AFN) for overnight growth. Resulting cultures were then diluted to 0.1 and grown in respective media to OD_{600} = 1. Based on previous CFU determinations, each culture was pelleted , washed once in PBS, and then resuspended in PBS to obtain 10^8 CFU/ml. Ten µl (10^6 CFUs) was administered by injection in the fourth proleg. To follow larvae mortality following *S. aureus* infection, 20 larvae were inoculated using 3 independent

cultures per culture condition (totaling 60 insects injected with SerFA, and 60 with SerFA-AFN), and 20 larvae were inoculated with PBS buffer for the control. Surviving larvae were counted every 24 h for 72 hours. To monitor *S. aureus* bacterial counts post-infection, the experiment above was repeated, and surviving larvae (9 total per condition, treated in 3 groups from independent biological replicates) were sacrificed until there were no surviving larvae left. CFUs were also determined from newly-dead larvae. To determine *S. aureus* CFUs, surviving larvae were chilled in ice for 30 min, and then crushed in 1 ml sterile deionized water. The resulting content was vortexed for ~30 sec. Five µl of 10-fold dilutions were prepared in sterile water and spotted on SerFA and SerFA-AFN solid medium. CFUs were determined after overnight incubation at 37°C. The detection threshold was 10^3 CFU per insect. Results of the 3 biologically independent experiments were pooled for presentation of insect mortality, and similarly for CFUs as done in a second independent experiment. Results are presented as the mean ± standard deviation (SD) using GraphPad Prism 9.3.1 (San Diego, Ca). CFU counts were compared by nonparametric t-test (Mann-Whitney U) ($P<0.05$). Note that *G. mellonella* naturally harbor enterococci (76). In contrast to *S. aureus*, enterococci are catalase-negative on routine plate tests (*n.b.*, some enterococci produce catalase upon heme addition). *S. aureus* were thus differentiated from enterococci on plates used for CFU enumeration by their catalase-positive response (*i.e.*, bubble formation) upon application of a 3% hydrogen peroxide solution. Enterococci did not produce bubbles.

Acknowledgments

The Nebraska Transposon Mutant Library strains were generously provided by BEI Resources, NIAID, NIH, USA. We acknowledge Micalis colleagues V. Sanchis and C. Nielson-LeRoux for valuable advice on the *G. mellonella* infection model, and C. Buisson for technical assistance, and access to the insectarium. L. Dupont provided excellent technical assistance in proteomic sample preparations. We thank our P. Gaudu for valuable discussions. We are grateful to Béatrice Py (CNRS UMR7283, Marseille, Fr) for pointing out the Fe-S cluster proteins in Staphylococci. F. Delolme (Université de Lyon) provided skillful assistance in phosphoproteome studies.

Funding

We gratefully acknowledge funding support from the French DIM 1-Health Project 00002247 (AG), the French National Research Agency StaphEscape project 16CE150013 (all authors), and the Fondation pour la Recherche Medicale (DBF20161136769)(AG). PW received a Franco-Thai scholarship from Campus France and Khon Kaen University. JPL and CG acknowledge financial support from the CNRS and the ITMO Cancer AVIESAN (Alliance Nationale pour les Sciences de la Vie et de la Santé, National Alliance for Life Sciences and Health) within the framework of the cancer plan for Orbitrap mass spectrometer funding. Phosphoproteomes were performed at the Protein Science Facility, SFR BioSciences CNRS UAR3444, Inserm US8, UCBL, ENS de Lyon, 50 Avenue Tony Garnier, 69007 Lyon, Fr.

Data Availability

All relevant data are within the manuscript and supporting information files.

Competing interests

The authors declare that no competing interests exist.

References

1. Lowy FD. *Staphylococcus aureus* infections. N Engl J Med. 1998;339(8):520-32.
2. Rasigade JP, Vandenesch F. *Staphylococcus aureus*: a pathogen with still unresolved issues. Infect Genet Evol. 2014;21:510-4.
3. Lakhundi S, Zhang K. Methicillin-Resistant *Staphylococcus aureus*: Molecular Characterization, Evolution, and Epidemiology. Clin Microbiol Rev. 2018;31(4).
4. Cusumano JA, Klinker KP, Huttner A, Luther MK, Roberts JA, LaPlante KL. Towards precision medicine: Therapeutic drug monitoring-guided dosing of vancomycin and beta-lactam antibiotics to maximize effectiveness and minimize toxicity. Am J Health Syst Pharm. 2020;77(14):1104-12.
5. Wang J, Soisson SM, Young K, Shoop W, Kodali S, Galgoci A, et al. Platensimycin is a selective FabF inhibitor with potent antibiotic properties. Nature. 2006;441(7091):358-61.
6. Wright HT, Reynolds KA. Antibacterial targets in fatty acid biosynthesis. Curr Opin Microbiol. 2007;10(5):447-53.
7. Karlowsky JA, Kaplan N, Hafkin B, Hoban DJ, Zhanel GG. AFN-1252, a FabI inhibitor, demonstrates a Staphylococcus-specific spectrum of activity. Antimicrob Agents Chemother. 2009;53(8):3544-8.
8. Brinster S, Lamberet G, Staels B, Trieu-Cuot P, Gruss A, Poyart C. Type II fatty acid synthesis is not a suitable antibiotic target for Gram-positive pathogens. Nature. 2009;458(7234):83-6.
9. Gloux K, Guillemet M, Soler C, Morvan C, Halpern D, Pourcel C, et al. Clinical Relevance of Type II Fatty Acid Synthesis Bypass in *Staphylococcus aureus*. Antimicrob Agents Chemother. 2017;61(5):61:e02515-16.
10. Kenanian G, Morvan C, Weckel A, Pathania A, Anba-Mondoloni J, Halpern D, et al. Permissive Fatty Acid Incorporation Promotes Staphylococcal Adaptation to FASII Antibiotics in Host Environments. Cell Rep. 2019;29(12):3974-82 e4.
11. Morvan C, Halpern D, Kenanian G, Hays C, Anba-Mondoloni J, Brinster S, et al. Environmental fatty acids enable emergence of infectious *Staphylococcus aureus* resistant to FASII-targeted antimicrobials. Nat Commun. 2016;7:12944.
12. Pishchany G, Mevers E, Ndousse-Fetter S, Horvath DJ, Jr., Paludo CR, Silva-Junior EA, et al. Amycomicin is a potent and specific antibiotic discovered with a targeted interaction screen. Proc Natl Acad Sci U S A. 2018;115(40):10124-9.
13. Yao J, Rock CO. Resistance Mechanisms and the Future of Bacterial Enoyl-Acyl Carrier Protein Reductase (FabI) Antibiotics. Cold Spring Harb Perspect Med. 2016;6(3):a027045.
14. Fage CD, Lathouwers T, Vanmeert M, Gao LJ, Vrancken K, Lammens EM, et al. The Kalimantacin Polyketide Antibiotics Inhibit Fatty Acid Biosynthesis in *Staphylococcus aureus* by Targeting the Enoyl-Acyl Carrier Protein Binding Site of FabI. Angew Chem Int Ed Engl. 2020;59(26):10549-56.
15. Parker EN, Cain BN, Hajian B, Ulrich RJ, Geddes EJ, Barkho S, et al. An Iterative Approach Guides Discovery of the FabI Inhibitor Fabimycin, a Late-Stage Antibiotic Candidate with In Vivo Efficacy against Drug-Resistant Gram-Negative Infections. ACS Cent Sci. 2022;8(8):1145-58.
16. Parsons JB, Frank MW, Subramanian C, Saenkham P, Rock CO. Metabolic basis for the differential susceptibility of Gram-positive pathogens to fatty acid synthesis inhibitors. Proc Natl Acad Sci U S A. 2011;108(37):15378-83.
17. Mader U, Nicolas P, Depke M, Pane-Farre J, Debarbouille M, van der Kooi-Pol MM, et al. *Staphylococcus aureus* Transcriptome Architecture: From Laboratory to Infection-Mimicking Conditions. PLoS Genet. 2016;12(4):e1005962.
18. Hamamoto H, Panthee S, Paudel A, Ohgi S, Suzuki Y, Makimura K, et al. Transcriptome change of *Staphylococcus aureus* in infected mouse liver. Commun Biol. 2022;5(1):721.
19. Lacey RW, Lord VL. Sensitivity of staphylococci to fatty acids: novel inactivation of linolenic acid by serum. J Med Microbiol. 1981;14(1):41-9.
20. Litus EA, Permyakov SE, Uversky VN, Permyakov EA. Intrinsically Disordered Regions in Serum Albumin: What Are They For? Cell Biochem Biophys. 2018;76(1-2):39-57.
21. Lopez MS, Tan IS, Yan D, Kang J, McCreary M, Modrusan Z, et al. Host-derived fatty acids activate type VII secretion in *Staphylococcus aureus*. Proc Natl Acad Sci U S A. 2017;114(42):11223-8.

22.Alnaseri H, Arsic B, Schneider JE, Kaiser JC, Scinocca ZC, Heinrichs DE, et al. Inducible Expression of a Resistance-Nodulation-Division-Type Efflux Pump in *Staphylococcus aureus* Provides Resistance to Linoleic and Arachidonic Acids. J Bacteriol. 2015;197(11):1893-905.
23.Alnaseri H, Kuiack RC, Ferguson KA, Schneider JET, Heinrichs DE, McGavin MJ. DNA Binding and Sensor Specificity of FarR, a Novel TetR Family Regulator Required for Induction of the Fatty Acid Efflux Pump FarE in *Staphylococcus aureus*. J Bacteriol. 2019;201(3).
24.Huang L, Matsuo M, Calderon C, Fan SH, Ammanath AV, Fu X, et al. Molecular Basis of Rhodomyrtone Resistance in *Staphylococcus aureus*. mBio. 2022:e0383321.
25.Soares da Costa TP, Tieu W, Yap MY, Pendini NR, Polyak SW, Sejer Pedersen D, et al. Selective inhibition of biotin protein ligase from *Staphylococcus aureus*. J Biol Chem. 2012;287(21):17823-32.
26.Zuhlke D, Dorries K, Bernhardt J, Maass S, Muntel J, Liebscher V, et al. Costs of life - Dynamics of the protein inventory of *Staphylococcus aureus* during anaerobiosis. Sci Rep. 2016;6:28172.
27.Pathania A, Anba-Mondoloni J, Gominet M, Halpern D, Dairou J, Dupont L, et al. (p)ppGpp/GTP and Malonyl-CoA Modulate *Staphylococcus aureus* Adaptation to FASII Antibiotics and Provide a Basis for Synergistic Bi-Therapy. mBio. 2021;12(1).
28.Singh VK, Syring M, Singh A, Singhal K, Dalecki A, Johansson T. An insight into the significance of the DnaK heat shock system in *Staphylococcus aureus*. Int J Med Microbiol. 2012;302(6):242-52.
29.Liu GY, Essex A, Buchanan JT, Datta V, Hoffman HM, Bastian JF, et al. *Staphylococcus aureus* golden pigment impairs neutrophil killing and promotes virulence through its antioxidant activity. J Exp Med. 2005;202(2):209-15.
30.Mosel M, Li L, Drlica K, Zhao X. Superoxide-mediated protection of Escherichia coli from antimicrobials. Antimicrob Agents Chemother. 2013;57(11):5755-9.
31.Gerstel A, Zamarreno Beas J, Duverger Y, Bouveret E, Barras F, Py B. Oxidative stress antagonizes fluoroquinolone drug sensitivity via the SoxR-SUF Fe-S cluster homeostatic axis. PLoS Genet. 2020;16(11):e1009198.
32.Schurig-Briccio LA, Parraga Solorzano PK, Lencina AM, Radin JN, Chen GY, Sauer JD, et al. Role of respiratory NADH oxidation in the regulation of *Staphylococcus aureus* virulence. EMBO Rep. 2020;21(5):e45832.
33.Cole J, Aberdein J, Jubrail J, Dockrell DH. The role of macrophages in the innate immune response to Streptococcus pneumoniae and *Staphylococcus aureus*: mechanisms and contrasts. Adv Microb Physiol. 2014;65:125-202.
34.Mayer-Scholl A, Averhoff P, Zychlinsky A. How do neutrophils and pathogens interact? Curr Opin Microbiol. 2004;7(1):62-6.
35.Garcia-Garcia T, Poncet S, Derouiche A, Shi L, Mijakovic I, Noirot-Gros MF. Role of Protein Phosphorylation in the Regulation of Cell Cycle and DNA-Related Processes in Bacteria. Front Microbiol. 2016;7:184.
36.Mijakovic I, Grangeasse C, Turgay K. Exploring the diversity of protein modifications: special bacterial phosphorylation systems. FEMS Microbiol Rev. 2016;40(3):398-417.
37.Derouiche A, Bidnenko V, Grenha R, Pigonneau N, Ventroux M, Franz-Wachtel M, et al. Interaction of bacterial fatty-acid-displaced regulators with DNA is interrupted by tyrosine phosphorylation in the helix-turn-helix domain. Nucleic Acids Res. 2013;41(20):9371-81.
38.Prust N, van der Laarse S, van den Toorn H, van Sorge NM, Lemeer S. In depth characterization of the *Staphylococcus aureus* phosphoproteome reveals new targets of Stk1. Mol Cell Proteomics. 2021:100034.
39.Albanesi D, Reh G, Guerin ME, Schaeffer F, Debarbouille M, Buschiazzo A, et al. Structural basis for feed-forward transcriptional regulation of membrane lipid homeostasis in *Staphylococcus aureus*. PLoS Pathog. 2013;9(1):e1003108.
40.Roux CM, DeMuth JP, Dunman PM. Characterization of components of the *Staphylococcus aureus* mRNA degradosome holoenzyme-like complex. J Bacteriol. 2011;193(19):5520-6.
41.Khemici V, Prados J, Petrignani B, Di Nolfi B, Berge E, Manzano C, et al. The DEAD-box RNA helicase CshA is required for fatty acid homeostasis in *Staphylococcus aureus*. PLoS Genet. 2020;16(7):e1008779.
42.Schujman GE, Paoletti L, Grossman AD, de Mendoza D. FapR, a bacterial transcription factor involved in global regulation of membrane lipid biosynthesis. Dev Cell. 2003;4(5):663-72.

43.Chastanet A, Fert J, Msadek T. Comparative genomics reveal novel heat shock regulatory mechanisms in *Staphylococcus aureus* and other Gram-positive bacteria. Mol Microbiol. 2003;47(4):1061-73.
44.Said-Salim B, Dunman PM, McAleese FM, Macapagal D, Murphy E, McNamara PJ, et al. Global regulation of *Staphylococcus aureus* genes by Rot. J Bacteriol. 2003;185(2):610-9.
45.Lei MG, Lee CY. Repression of Capsule Production by XdrA and CodY in *Staphylococcus aureus*. J Bacteriol. 2018;200(18).
46.McCallum N, Hinds J, Ender M, Berger-Bachi B, Stutzmann Meier P. Transcriptional profiling of XdrA, a new regulator of spa transcription in *Staphylococcus aureus*. J Bacteriol. 2010;192(19):5151-64.
47.DeFrancesco AS, Masloboeva N, Syed AK, DeLoughery A, Bradshaw N, Li GW, et al. Genome-wide screen for genes involved in eDNA release during biofilm formation by *Staphylococcus aureus*. Proc Natl Acad Sci U S A. 2017;114(29):E5969-E78.
48.Ding Y, Liu X, Chen F, Di H, Xu B, Zhou L, et al. Metabolic sensor governing bacterial virulence in *Staphylococcus aureus*. Proc Natl Acad Sci U S A. 2014;111(46):E4981-90.
49.Geiger T, Goerke C, Mainiero M, Kraus D, Wolz C. The virulence regulator Sae of *Staphylococcus aureus*: promoter activities and response to phagocytosis-related signals. J Bacteriol. 2008;190(10):3419-28.
50.Ericson ME, Subramanian C, Frank MW, Rock CO. Role of Fatty Acid Kinase in Cellular Lipid Homeostasis and SaeRS-Dependent Virulence Factor Expression in *Staphylococcus aureus*. mBio. 2017;8(4).
51.Kazek M, Kaczmarek A, Wronska AK, Bogus MI. Dodecanol, metabolite of entomopathogenic fungus Conidiobolus coronatus, affects fatty acid composition and cellular immunity of Galleria mellonella and Calliphora vicina. Sci Rep. 2021;11(1):15963.
52.Hunt T, Kaplan N, Hafkin B. Safety, tolerability and pharmacokinetics of multiple oral doses of AFN-1252 administered as immediate release (IR) tablets in healthy subjects. Journal of chemotherapy. 2016;28(3):164-71.
53.Banevicius MA, Kaplan N, Hafkin B, Nicolau DP. Pharmacokinetics, pharmacodynamics and efficacy of novel FabI inhibitor AFN-1252 against MSSA and MRSA in the murine thigh infection model. Journal of chemotherapy. 2013;25(1):26-31.
54.Escaich S, Prouvensier L, Saccomani M, Durant L, Oxoby M, Gerusz V, et al. The MUT056399 inhibitor of FabI is a new antistaphylococcal compound. Antimicrob Agents Chemother. 2011;55(10):4692-7.
55.DeCoursey TE. During the respiratory burst, do phagocytes need proton channels or potassium channels, or both? Sci STKE. 2004;2004(233):pe21.
56.Ezraty B, Vergnes A, Banzhaf M, Duverger Y, Huguenot A, Brochado AR, et al. Fe-S cluster biosynthesis controls uptake of aminoglycosides in a ROS-less death pathway. Science. 2013;340(6140):1583-7.
57.Slack FJ, Serror P, Joyce E, Sonenshein AL. A gene required for nutritional repression of the Bacillus subtilis dipeptide permease operon. Mol Microbiol. 1995;15(4):689-702.
58.Waters NR, Samuels DJ, Behera RK, Livny J, Rhee KY, Sadykov MR, et al. A spectrum of CodY activities drives metabolic reorganization and virulence gene expression in *Staphylococcus aureus*. Mol Microbiol. 2016;101(3):495-514.
59.Zhou C, Bhinderwala F, Lehman MK, Thomas VC, Chaudhari SS, Yamada KJ, et al. Urease is an essential component of the acid response network of *Staphylococcus aureus* and is required for a persistent murine kidney infection. PLoS Pathog. 2019;15(1):e1007538.
60.Tuchscherr L, Loffler B, Proctor RA. Persistence of *Staphylococcus aureus*: Multiple Metabolic Pathways Impact the Expression of Virulence Factors in Small-Colony Variants (SCVs). Front Microbiol. 2020;11:1028.
61.Peyrusson F, Nguyen TK, Najdovski T, Van Bambeke F. Host Cell Oxidative Stress Induces Dormant *Staphylococcus aureus* Persisters. Microbiol Spectr. 2022;10(1):e0231321.
62.Painter KL, Strange E, Parkhill J, Bamford KB, Armstrong-James D, Edwards AM. *Staphylococcus aureus* adapts to oxidative stress by producing H2O2-resistant small-colony variants via the SOS response. Infect Immun. 2015;83(5):1830-44.
63.Sendi P, Proctor RA. *Staphylococcus aureus* as an intracellular pathogen: the role of small colony variants. Trends Microbiol. 2009;17(2):54-8.
64.Kriegeskorte A, Konig S, Sander G, Pirkl A, Mahabir E, Proctor RA, et al. Small colony variants of *Staphylococcus aureus* reveal distinct protein profiles. Proteomics. 2011;11(12):2476-90.

65.Fey PD, Endres JL, Yajjala VK, Widhelm TJ, Boissy RJ, Bose JL, et al. A genetic resource for rapid and comprehensive phenotype screening of nonessential *Staphylococcus aureus* genes. MBio. 2013;4(1):e00537-12.
66.McMurry LM, Oethinger M, Levy SB. Triclosan targets lipid synthesis. Nature. 1998;394(6693):531-2.
67.Morvan C, Halpern D, Kenanian G, Pathania A, Anba-Mondoloni J, Lamberet G, et al. The *Staphylococcus aureus* FASII bypass escape route from FASII inhibitors. Biochimie. 2017;141:40-6.
68.Bednarz B, Millan-Oropeza A, Kotowska M, Swiat M, Quispe Haro JJ, Henry C, et al. Coelimycin Synthesis Activatory Proteins Are Key Regulators of Specialized Metabolism and Precursor Flux in Streptomyces coelicolor A3(2). Front Microbiol. 2021;12:616050.
69.Boersema PJ, Raijmakers R, Lemeer S, Mohammed S, Heck AJ. Multiplex peptide stable isotope dimethyl labeling for quantitative proteomics. Nat Protoc. 2009;4(4):484-94.
70.Soufi B, Taumer C, Semanjski M, Macek B. Phosphopeptide Enrichment from Bacterial Samples Utilizing Titanium Oxide Affinity Chromatography. Methods Mol Biol. 2018;1841:231-47.
71.The M, MacCoss MJ, Noble WS, Kall L. Fast and Accurate Protein False Discovery Rates on Large-Scale Proteomics Data Sets with Percolator 3.0. J Am Soc Mass Spectrom. 2016;27(11):1719-27.
72.Zierdt CH, Golde DW. Deoxyribonuclease-positive Staphylococcus epidermidis strains. Appl Microbiol. 1970;20(1):54-7.
73.Park JH, Lee JH, Cho MH, Herzberg M, Lee J. Acceleration of protease effect on *Staphylococcus aureus* biofilm dispersal. FEMS Microbiol Lett. 2012;335(1):31-8.
74.Araiza-Villanueva M, Avila-Calderon ED, Flores-Romo L, Calderon-Amador J, Sriranganathan N, Qublan HA, et al. Proteomic Analysis of Membrane Blebs of Brucella abortus 2308 and RB51 and Their Evaluation as an Acellular Vaccine. Front Microbiol. 2019;10:2714.
75.Sheehan G, Dixon A, Kavanagh K. Utilization of Galleria mellonella larvae to characterize the development of *Staphylococcus aureus* infection. Microbiology (Reading). 2019;165(8):863-75.
76.Allonsius CN, Van Beeck W, De Boeck I, Wittouck S, Lebeer S. The microbiome of the invertebrate model host Galleria mellonella is dominated by Enterococcus. Anim Microbiome. 2019;1(1):7.

Table 1. Regulatory proteins showing changes in phosphorylation during anti-FASII adaptation.

Accession number	Name	Function	Phosphorylation site[a]	Abundance ratio[b]		
				SerFA-Tric6h /SFA	SerFA-Tric10h /SFA	SerFA-Tric10h /SerFA-Tric6h
SAUSA300_0658	CcpE	Transcriptional regulator, LysR family	$_{8}$LLI**T**LDETK$_{16}$	0.34	0.23	0.39
SAUSA300_1448	Fur	Transcriptional regulator	$_{24}$EA**T**VRVLIENEK$_{35}$	N.d.	100	100
SAUSA300_1542	HrcA	Heat-inducible transcription repressor	$_{260}$IAELLQDI**SS**PNINVK$_{275}$	100	100	0.04
SAUSA300_1708	Rot	HTH-type transcriptional regulator repressor of toxins	$_{4}$LAHTSFGIVGMFVN**T**CIVAK$_{23}$	0.01	3.91	100
SAUSA300_1797	XdrA	HTH-cro/C1-type domain-containing protein	$_{116}$V**S**NI**Y**RVLNPDNQPIFGTSK$_{135}$	2.96	0.01	0.01

[a] Peptide positions in the protein sequence are indicated. Phosphorylated amino-acids are in bold red letters, or in bold black when there is an ambiguity. [b] An abundance ratio of 100 means that the protein was detected only in the numerator, but not the denominator condition. A ratio of 0.01 means that the protein was found only in the denominator, and not in the numerator condition. N.d., signals for SerFA-Tric 6h and SerFA are below detection levels.

Table 2. Anti-FASII-adapted *S. aureus* remain adapted during insect infection [a].

Plating medium	CFU (standard deviation) from live larvae							
	Non-treated *S. aureus*				Anti-FASII-adapted *S. aureus* [b]			
	0h	24h	48h	72h	0h	24h	48h	72h
SerFA	$1.5x10^6$ ($\pm 1.3 \times 10^6$) N=9	$8.8x10^8$ ($\pm 6.8x10^8$) N=9	†	†	1.2×10^5 ($\pm 0.7 \times 10^5$) N=9	$2.8x10^8$ ($\pm 3.4 \times 10^8$) N=9 (1 without *S. aureus*)	$3.4x10^7$ ($\pm 3.6 \times 10^7$) N=9	$4.7x10^6$ ($\pm 9.7x10^6$) N=8 (1 without *S. aureus*)
SerFA-AFN	No growth N=9	No growth N=9	†	†	$8.7x10^5$ ($\pm 5.6 \times 10^5$) N=9	$2.7x10^8$ ($\pm 2.6 \times 10^8$) N=9 (1 without *S. aureus*)	$1.2x10^8$ ($\pm 1.6 \times 10^8$) N=9	$2.3x10^6$ ($\pm 4.0 \times 10^6$) N=8 (2 without *S. aureus* [c])

	CFU (standard deviation) from dead larvae	
Plating medium	Non-treated *S. aureus*	Anti-FASII adapted *S. aureus*
	48h	48h
SerFA	$9.0x10^9$ ($\pm 8.7 \times 10^9$) N=9	$1.4x10^{10}$ ($\pm 1.5 \times 10^{10}$) N=8
SerFA-AFN	No growth N=9	$1.6x10^{10}$ ($\pm 2.0 \times 10^{10}$) N=8

[a] CFUs of infected surviving (upper) and dead (lower) insects were compared on SerFA and SerFA-AFN solid medium. Anti-FASII-adapted *S. aureus* are distinguished from non-treated bacteria by their ability to form colonies on SerFA-AFN. [b] Individuals without detectable CFU ($<10^3$ CFU per insect) in SerFA or SerFA-AFN, or only on SerFA-AFN plates, are indicated. [c] Bacteria in one individual were no longer anti-FASII-adapted, and failed to grow on SerFA-AFN. †, no surviving insects. N= number of insects for each time point.

Figure Legends

Fig. 1. Expression changes related to *S. aureus* anti-FASII adaptation. Normalized protein expression profiles are organized by growth condition (BHI, FA, SerFA) without and with triclosan (Materials and Methods). **A.** Heat map of global protein changes induced during *S. aureus* adaptation to FASII inhibitor triclosan. **B.** Heat map of condition-specific highly expressed proteins. Proteins listed at right of heat map show high differential expression in conditions indicated after the bracket. Gene names and conditions of highest abundance are at right. FA-Tric and SerFA-Tric kinetics samples were each considered as a group regardless of the time of increased expression. Hyp, hypothetical protein. Color code: Light-to-dark shades of grey, green, and pink represent respectively BHI ± Tric, FA ± Tric, SerFA ± Tric as indicated. Incremental 2, 4, 6, 8, and 10 h time points for FA-Tric and for SerFA-Tric are represented by wedges. The heat map scale is at lower left: representations are calculated as relative protein abundance ratios (red, up-represented; blue, down-represented).

Fig. 2. Heat map of FASII and phospholipid synthesis proteins whose expression is affected in SerFA-Tric growth. Proteins were compiled based on confirmed FASII and phospholipid synthesis pathway proteins. FabI (FASII; SAUSA300_0912) and PlsY (phospholipid synthesis; SAUSA300_1249) were not detected in this proteome. Results are limited to SerFA (control) and SerFA-Tric adaptation conditions. See **S1 Table** for results in all test conditions. Gene names and functional categories are at right. Incremental time points for SerFA-Tric 2, 4, 6, 8, and 10 h samples are represented by the wedge. The heat map scale is at lower right: representations are calculated as relative protein abundance ratios (red, up-represented; blue, down-represented).

Fig. 3. Stress response proteins are up-expressed during anti-FASII adaptation. Heat maps are shown for known or putative stress response proteins. Results are limited to SerFA (control) and SerFA-Tric adaptation conditions. See **S1 Table** for results in all test conditions. Gene names and functional

categories are at right. Incremental time points for SerFA-Tric 2, 4, 6, 8, and 10 h samples are represented by the wedge. The heat map scale is at lower right: representations are calculated as relative protein abundance ratios (red, up-represented; blue, down-represented).

Fig. 4. H_2O_2 primes bacteria for accelerated adaptation to anti-FASII. A. *S. aureus* anti-FASII adaptation leads to increased H_2O_2 resistance. USA300 non-treated (black bar) and AFN-1252-adapted cultures (hatched bar) issued from overnight growth were challenged with 0.5 mM H_2O_2. CFUs of surviving bacteria and controls were determined after 5 h incubation. **B.** and **C.** Priming *S. aureus* with H_2O_2 accelerates anti-FASII adaptation. **B.** USA300 cultures were grown overnight in SerFA without or with 0.5 mM H_2O_2. Cultures were diluted to OD_{600} = 0.1 and grown without or with 0.5 µg/ml AFN-1252. OD_{600} was monitored for 12 h. Growth curve is representative of 4 independent experiments. Black, no pretreatment; purple, pre-treatment with H_2O_2. Solid lines, SerFA, dashed lines SerFA-AFN. **C.** FA profiles were done twice independently on cultures harvested after 6 h anti-FASII treatment (arrow in '**B**'). 1, 2, and 3, eFAs added to cultures (respectively C14, C16, and C18:1). H_2O_2-primed cultures incorporate more eFAs than unprimed cultures. See Materials and Methods for protocols.

Fig. 5. Decreases in virulence factor levels and activities in anti-FASII adapted *S. aureus*. A. Heat maps are shown for known virulence factors. Results are limited to SerFA (control) and SerFA-Tric adaptation conditions. See **S1 Table** for results in all test conditions. Gene names and functional categories are at right. Incremental time points for SerFA-Tric 2, 4, 6, 8, and 10 h samples are represented by the wedge. The heat map scale is at lower right: representations are calculated as relative protein abundance ratios (red, up-represented; blue, down-represented). **B.** Secreted virulence factor activities. Non-treated (NT) and anti-FASII-adapted cultures using Triclosan (Tric-ad) or AFN-1252 (AFN-ad) were grown overnight, and reached similar OD_{600} values (= 13, 9, and 9 respectively for NT, Tric-ad, and to AFN-ad). Cultures (for protease detection) and culture supernatants (hemolysin, lipase, and nuclease

detection) were evaluated (see Materials and Methods). A representative result of 3 biologically independent replicates is shown.

Fig. 6. **Regulatory proteins showing expression reversal in anti-FASII compared to non-treated cultures.** Heat maps are shown for known or putative regulators in public databases and were curated manually. Results are limited to SerFA control and SerFA-Tric adaptation conditions (see **S1 Table** for results in all test conditions). The greatest changes in most regulatory protein levels were visible at 6 and 8 h during the latency phase of anti-FASII adaptation. Gene names are at right. Incremental time points for SerFA-Tric 2, 4, 6, 8, and 10 h samples are represented by the wedge. The heat map scale is at lower right: representations are calculated as relative protein abundance ratios (red, up-represented; blue, down-represented). Regulators in bold displayed lasting shifts in anti-FASII adapted bacteria.

Fig. 7. Comparison of untreated and anti-FASII-treated *S. aureus* in a *G. mellonella* infection model. *S. aureus* cultures were prepared as described in Materials and Methods. Ten microliters were injected per insect. **A.** Insect mortality in non-treated and anti-FASII-adapted *S. aureus*. Data was analyzed using Kaplan-Meier with pooled values of biologically independent triplicates (60 samples per condition). A Mantel-Cox test was done on results excluding the PBS controls, and showed a significance value of $p < 0.0001$. **B.** Bacterial CFUs in insects infected by non-treated and anti-FASII-adapted *S. aureus* in surviving insects. †, no surviving insects. **C.** Bacterial CFUs in insects infected by non-treated and anti-FASII-adapted *S. aureus* in dead insects at 48 h. '**B**' and '**C**' analyses were done using the non-parametric Mann Whitney test using Graphpad prism software.

Fig. 8. Consequences of anti-FASII on *S. aureus* adaptation. Non-treated *S. aureus* synthesizes fatty acids (FAs) used to produce membrane phospholipids. A typical gas chromatography FA profile of *S. aureus* grown in laboratory medium (black line) is shown above a depiction of the membrane. Addition

of anti-FASII in SerFA medium results in a replacement of self-synthesized FAs by the eFAs (here C14, C16, C18:1; green line depicts bacterial profile), and an exogenous membrane phospholipid composition. Anti-FASII adaptation is accompanied by massive changes in protein expression. Notably, increases in numerous stress response proteins may help bacteria cope with host-produced ROS (55). Decreased virulence factor production may help bacteria avoid induction of the host immune response (60). Reservoirs of anti-FASII-adapted *S. aureus* may favor the emergence of *S. aureus* populations that persist in the host.

Supporting Information.

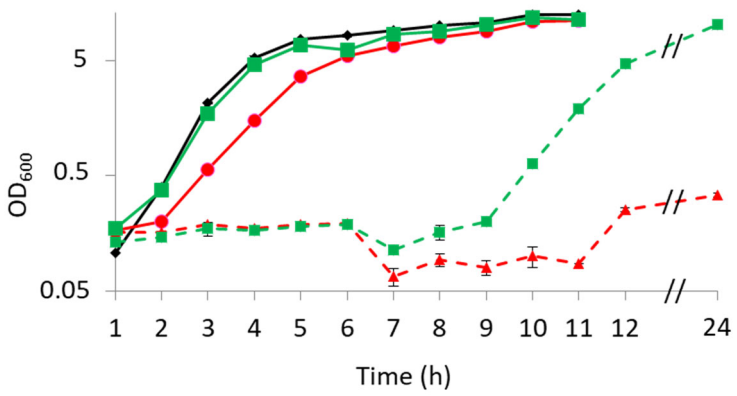

S1 Fig. Growth kinetics of USA300 in the absence and presence of the anti-FASII drug triclosan. USA300 growth in BHI and in SerFA medium follows equivalent kinetics. Growth in BHI (black), FA (red solid), SerFA (green solid), FA-Tric (red dashed), SerFA-Tric (green dashed). Adapted from (10)**.**

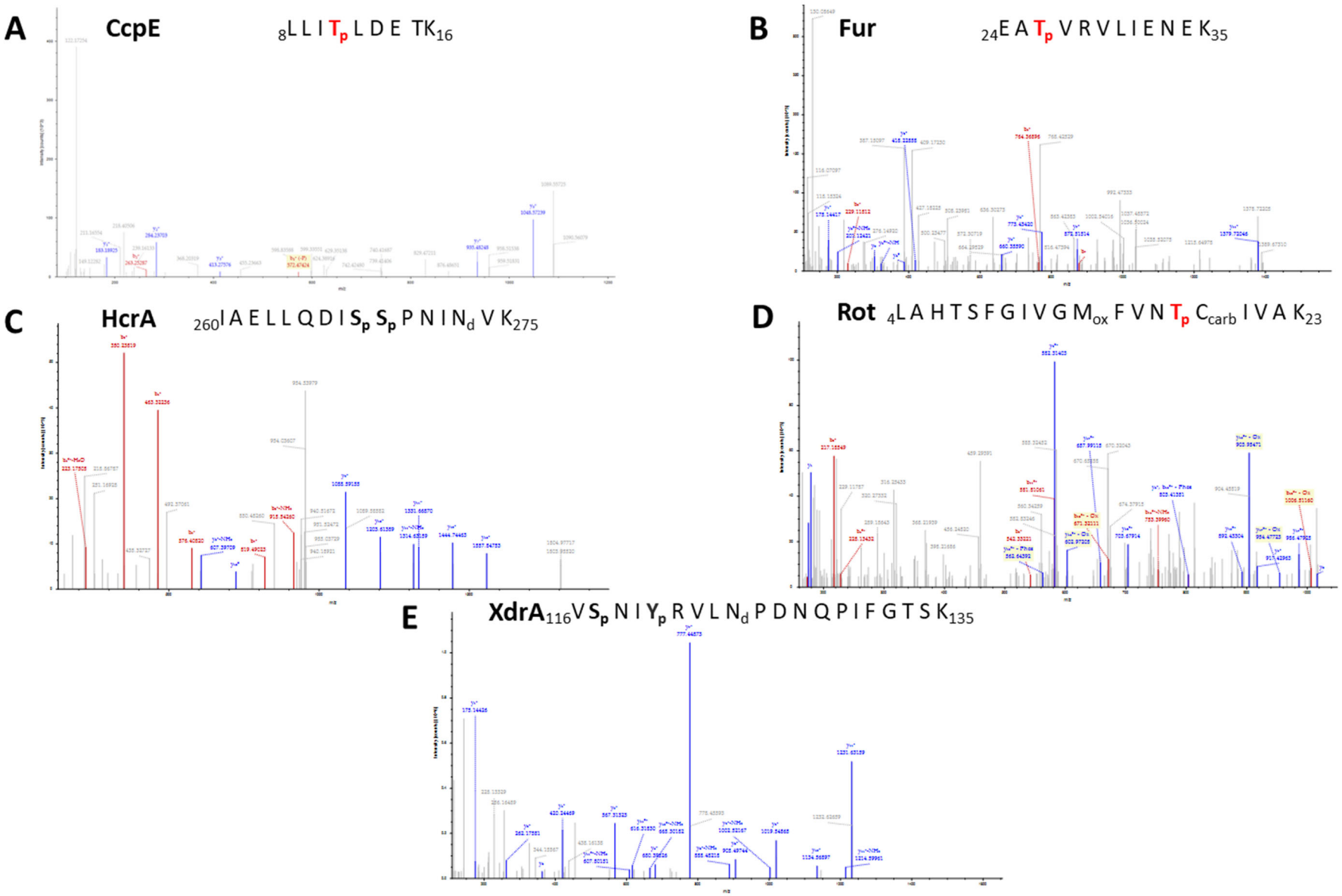

Fig. S2. Tandem Mass spectra of identifying differentially expressed phosphorylation sites of CcpE (A), Fur (B), HcrA (C), Rot (D) and XdrA (E) proteins. The identified phosphorylation sites are indicated in bold red when localization is validated and bold black when 2 phosphorylation sites are possible. d: deamidation, carb: carbamidomethylation, ox: oxidation, p: phosphorylation. All peptides are labeled by dimethyl tag on peptide N-term and lysines (K).

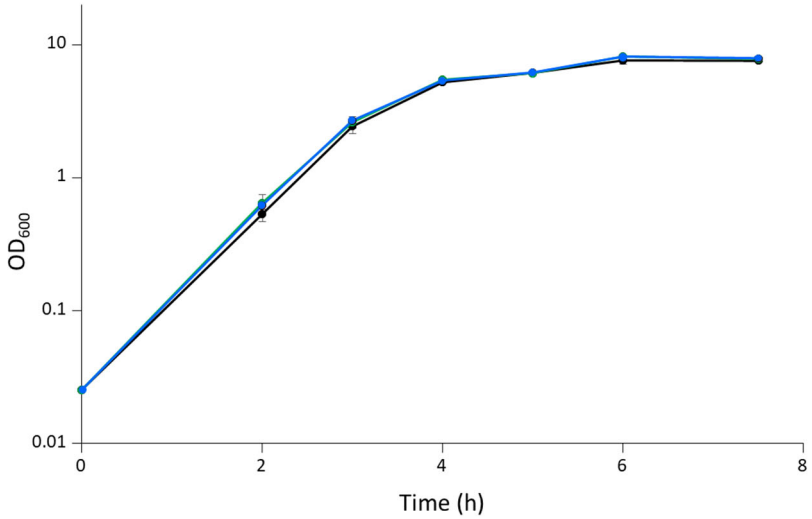

S3 Fig. *S. aureus* USA300 non-treated and anti-FASII-adapted cultures grow identically in non-selective SerFA medium. Overnight non-treated (black) and anti-FASII adapted *S. aureus* using triclosan (0.5 µg/ml; SerFA-Tric, green), or AFN-1252 (0.5 µg/ml; SerFA-AFN, blue), were diluted to OD_{600} 0.025 and grown in SerFA (non-selective) medium. Shown are the mean and standard deviation of independent triplicate replicates.

S1 Table. Proteomics of non-treated and anti-FASII (triclosan)-treated *S. aureus*: a kinetics study. Conditions, full results, cluster analysis.

S2 Table. Phosphorylated targets affected by anti-FASII adaptation. Full results.

S3 Table. Pre-treatments with ROS-generating *versus* reducing agents respectively accelerate and retard adaptation to anti-FASII.